Fractional Quantum Hall States at ν=13/5 and 12/5 and Their Non-Abelian Nature

W. Zhu, S. S. Gong, F. D. M. Haldane, and D. N. Sheng

Phys. Rev. Lett. **115**, 126805 — Published 18 September 2015

DOI: 10.1103/PhysRevLett.115.126805

The Fractional Quantum Hall States at $\nu = 13/5$ and $12/5$ and their Non-Abelian Nature

W. Zhu[1,2], S. S. Gong[2], F. D. M. Haldane[1] and D. N. Sheng[2]
[1]*Department of Physics, Princeton University, Princeton, NJ 08544, USA and*
[2]*Department of Physics and Astronomy, California State University, Northridge, CA 91330, USA*

Topological quantum states with non-Abelian Fibonacci anyonic excitations are widely sought after for the exotic fundamental physics they would exhibit, and for universal quantum computing applications. The fractional quantum Hall (FQH) state at filling factor $\nu = 12/5$ is a promising candidate, however, its precise nature is still under debate and no consensus has been achieved so far. Here, we investigate the nature of the FQH $\nu = 13/5$ state and its particle-hole conjugate state at $12/5$ with the Coulomb interaction, and address the issue of possible competing states. Based on a large-scale density-matrix renormalization group (DMRG) calculation in spherical geometry, we present evidence that the essential physics of the Coulomb ground state (GS) at $\nu = 13/5$ and $12/5$ is captured by the $k = 3$ parafermion Read-Rezayi state (RR_3), including a robust excitation gap and the topological fingerprint from entanglement spectrum and topological entanglement entropy. Furthermore, by considering the infinite-cylinder geometry (topologically equivalent to torus geometry), we expose the non-Abelian GS sector corresponding to a Fibonacci anyonic quasiparticle, which serves as a signature of the RR_3 state at $13/5$ and $12/5$ filling numbers.

Introduction.— While fundamental particles in nature are either bosons or fermions, the emergent excitations in two-dimensional strongly-correlated systems may obey fractional or anyonic statistics [1, 2]. After two decades of study [3–13], current interest in exotic excitations focuses on states of matter with non-Abelian quasiparticle excitations [14–16], and their potential applications to the rapidly evolving field of quantum computation and cryptography [17–22]. So far the most promising platform for realization of non-Abelian statistics is the fractional quantum Hall (FQH) effect in the first excited Landau level, and two of the most interesting examples are at filling factors $\nu = 5/2$ and $12/5$. The $\nu = 5/2$ state is widely considered to be the candidate for the Moore-Read state hosting non-Abelian Majorana quasiparticles [14–16]. Experiments have revealed that the $12/5$ state appears to behave differently from the conventional FQH effect [5, 8], and may also be a candidate state for hosting non-Abelian excitations. However, the exact nature of the FQH $12/5$ state is still undetermined due to the existence of other possible competing candidate states.

Several ground-state (GS) wavefunctions have been proposed [16, 25, 29–32] as models for the observed FQH effect at $\nu = 12/5$ [5, 8, 13]. The most exciting candidate is the $k = 3$ parafermion state proposed by Read and Rezayi (RR_3)[16]. This RR_3 state describes a condensate of three-electron clusters that forms an incompressible state at $\nu = 13/5$ [16]. One can also construct the particle-hole partner of the RR_3 state to describe the $12/5$ FQH effect. Besides the RR_3 state, some competing candidates for $\nu = 13/5$ or $12/5$ exist: a hierarchy state [26, 27], a Jain composite-fermion (CF) state [28], a generalization of the non-Abelian Pfaffian state by Bonderson and Slingerland (BS) [29, 30], and a bipartite CF state [31, 32]. So far, the true nature of the $12/5$ and $13/5$ FQH states remains undetermined. The main challenges in settling this issue are the limited computational ability and the lack of an efficient diagnostic method. For example, from exact diagonalization (ED) calculations in the limited feasible range of system sizes, it is found that the overlaps between the Coulomb GS at $\nu = 12/5$ and different model wavefunctions are all relatively large [16, 30], while the extrapolated GS energies of the RR_3 and BS states are very close in the thermodynamic limit [30, 33]. Taken as a whole, previous studies have left the nature of the Coulomb GS at $\nu = 13/5$ and $12/5$ unsettled.

Recently, there has been growing interest in connecting quantum entanglement [34–37] with emergent topological order [38, 39] in strongly interacting systems, which offers a new route to identification of the precise topological order of a many-body state. Although characterization of entanglement has been successfully used to identify various well-known types of topological order [40–47], application of the method to a system with competing phases still faces challenges when ED studies suffer from strong finite size effects, and other methods such as quantum Monte-Carlo suffer from sign problems. The recent development of the high efficiency density-matrix renormalization group (DMRG) in momentum space [44, 54] allows the study of such systems in sphere and cylinder geometries, both of which can be used to make concrete predictions of the physics of real systems in the thermodynamic limit. Here we combine these advances, and use these two geometries to address the long-standing issues of the FQH at $\nu = 12/5$ and $13/5$.

In this paper, we study the FQH at $\nu = 12/5$ and $13/5$ filling by using the state-of-the-art density-matrix renormalization group (DMRG) numerical simulations. By studying large systems up to $N_e = 36$ on spherical geometry, we establish that the Coulomb GS at $\nu = 13/5$ is an incompressible FQH state, protected by a robust neutral excitation gap $\Delta_n \approx 0.012(e^2/l_B)$. Crucially, we show that the entanglement spectrum (ES) fits the corresponding $SU(2)_3$ conformal field theory (CFT) which describes the edge structure of the parafermion RR_3 state. The topological entanglement entropy (TEE) is also consistent with the predicted value for the RR_3 state, indicating the emergence of Fibonacci anyonic quasiparticles. Moreover, we also perform a finite-size scaling analysis of the GS energies for $\nu = 12/5$ states at different shifts corresponding to the particle-hole-conjugate of the RR_3 state, the Jain state and BS state. Finite-size scaling confirms that the ground state with topological shift $\mathcal{S} = -2(3)$ (where RR_3 and its particle-hole partner states are expected to occur) is energetically favored in the thermodynamic limit. Finally, to explicitly demonstrate the topological degeneracy, we obtain two topological distinct GS sectors on the infinite cylinder using infinite-size DMRG. While one sector is the identity sector matching to the GS from the sphere, the new sector is identified as the non-Abelian sector with a Fibonacci anyonic quasiparticle through its characteristic ES and TEE. Thus we establish that the essence of the FQH state at $\nu = 13/5$ is fully captured by the non-Abelian parafermion RR_3 state (and by its particle-hole conjugate at ν = 12/5) and show that it is stable against perturbations as we change the Haldane pseudopotentials and the layer width of the system.

Model and Method.— We use the Haldane representation [26, 48, 49] in which the N_e electrons are confined on the surface of a sphere surrounding a magnetic monopole of strength Q. In this case, the orbitals of the n-th LL are represented as orbitals with azimuthal angular momentum $-L, -L+1, ..., L$, with $L = Q + n$ being the total angular momentum. The total magnetic flux through the spherical surface is quantized to be an integer $N_s = 2L$. Assuming that electron spins are fully-polarized and neglecting Landau-level mixing, the Hamiltonian in the spherical geometry can be written as:

$$H = \frac{1}{2} \sum_{m_1+m_2=m_3+m_4} \langle m_1, m_2|V|m_3, m_4\rangle \hat{a}^\dagger_{m_1} \hat{a}^\dagger_{m_2} \hat{a}_{m_3} \hat{a}_{m_4}$$

where $\hat{a}^\dagger_m$ ($\hat{a}_m$) is the creation (annihilation) operator at the orbital m and V is the Coulomb interaction between electrons in units of e^2/l_B with l_B being the magnetic length. The two-body Coulomb interaction element can be decomposed as

$$\langle i, j|V|p, q\rangle = \sum_{l=0}^{2L} \sum_{m=-l}^{l} \langle L, i; L, j|l, m\rangle\langle l, m|L, p; L, q\rangle \mathcal{V}^n(l)$$

where $\langle L, i; L, j|l, m\rangle$ is the Clebsch-Gordan coefficients and $\mathcal{V}^n(l)$ is the Haldane pseudopotential representing the pair energy of two electrons with relative angular momentum $2L - l$ in n-th LL [26, 71]. For electrons at fractional filling factor ν, $N_s = \nu^{-1}N_e - \mathcal{S}$, where $\mathcal{S}$ is the curvature-induced "shift" on the sphere.

Our calculation is based on the unbiased DMRG method [50–55], combined with ED. The (angular) momentum-space DMRG allows us to use the total electron number N_e and the total z-component of angular momentum $L^{tot}_z = \sum_{i=1}^{N_e} m_i$ as good quantum numbers to reduce the Hilbert subspace dimension [54]. Here, we report the result at $\nu = 13/5(12/5)$ with electron number up to $N_e = 36(22)$ by keeping up to 30000 states with optimized DMRG, which allows us to obtain accurate results for energy and the ES on much larger system sizes beyond the ED limit ($N_e^{ED} = 24(16)$ at $\nu = 13/5(12/5)$).

Groundstate Energy, Energy Spectrum and Neutral Gap.— We first compute the GS energies for a number of systems up to $N_e = 36$ at $\nu = 13/5$, with a shift $\mathcal{S} = 3$ consistent with the RR_3 state. As shown in the low-lying energy spectrum in the inset of Fig. 1(b) obtained from ED for $N_e = 21$, the GS is located in the $L^{tot} = 0$ sector and is separated from the higher energy continuum by a finite gap, which signals an incompressible FQH state. The extrapolation of the GS energy to the thermodynamic limit can be carried out using a quadratic function of $1/N_e$ (blue line), or a linear fit in $1/N_e$ (red line) after renormalizing the energy by $\sqrt{2Q\nu/N_e}$ to take into account the curvature of the sphere [56], as shown in Fig. 1(a). We obtain the $E_0/N_e = -0.38458(24)$ (blue line) and $-0.38487(9)$ (red line), which demonstrates consistency between the two extrapolating schemes.

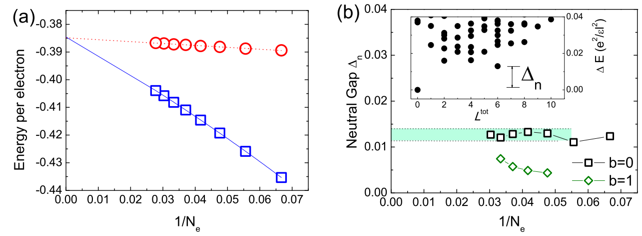

FIG. 1: (a) The groundstate energy per electron (blue dots) corresponding to the $\nu = 13/5$ state. The blue line shows the extrapolated values obtained using a quadratic function of $1/N_e$. The red dots shows the rescaling energy by a renormalized magnetic length and the red line is the linear fitting. (b) The neutral gap Δ_n for 13/5 state as a function of the $1/N_e$ (b is the layer-width parameter [71]). Inset: Energy spectrum versus total angular momentum L^{tot} for $N_e = 21$. Δ_n is defined as the energy difference between the lowest energy state (in $L^{tot} = 0$) and the first excited state (in $L^{tot} \neq 0$).

We also calculated the neutral excitation gap Δ_n at $\nu = 13/5$ [57]. This is equivalent to the energy difference between the GS and the "roton minimum"[58–60] as illustrated in the inset of Fig. 1(b). The roton minimum corresponds to the lowest excitation energy of a quasielectron-quasihole pair [60]. Fig. 1(b) shows Δ_n as a function of $1/N_e$, where the large-system results indicate that the neutral gap approaches a nonzero value $\Delta_n \approx 0.012 \pm 0.001$ for $N_e \geq 21$. Since the Hamiltonian in this paper is particle-hole symmetric, the neutral gap at $\nu = 12/5$ and $13/5$ are expected to be identical [61]. In addition, if the effect of finite layer-width is considered[71], the neutral-excitation gap is reduced but still remains consistent with a nonzero value (Fig. 1(b)).

Competing states.— In Fig. 2, we compare the GS energies per electron of three known candidates for $\nu = 12/5$: the particle-hole conjugate of the RR_3 state with a shift $\mathcal{S} = -2$, the non-Abelian BS state with $\mathcal{S} = 2$ [29], and Jain state with $\mathcal{S} = 4$. We find that the lowest-energy state for the Jain state shift ($\mathcal{S} = 4$) in larger system sizes has a total angular momentum $L^{tot} \neq 0$, indicating that it represents excitations of some other incompressible state rather than the Coulomb GS at $\nu = 12/5$ [32]. Secondly, the GSs with the RR_3 and BS shifts continue to have $L^{tot} = 0$ for the systems

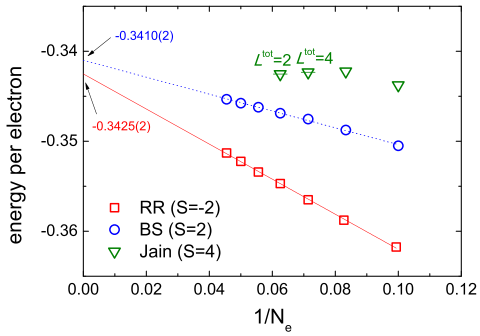

FIG. 2: Finite-size extrapolation of the ground-state (GS) energies for different shifts corresponding to different candidate states at $\nu = 12/5$. All energies have been rescaled by the renormalized magnetic length. The angular momentum of the GS is shown whenever it is nonzero ($L^{tot} \neq 0$).

that we have studied, and the extrapolation based on the result for $10 \leq N_e \leq 22$ leads to $E_0/N_e = -0.3425$ for the RR_3 state and $E_0/N_e = -0.3410$ for the BS state, respectively. Compared to the previous studies [30, 33], the extrapolation errors are reduced by the inclusion of larger system sizes obtained using DMRG. Our calculations suggest that the GS state with shift $\mathcal{S} = -2(\mathcal{S} = 3)$ is energetically favored at $\nu = 12/5(13/5)$. Our results are consistent with the interpretation that the RR_3 state describes the true GS (see the full evidence below), while the other states at nearby shifts correspond to states with quasiparticle or quasihole excitations.

Orbital ES.— Li and Haldane first established that the orbital ES of the GS of FQH phase contains information about the counting of their edge modes [36, 39]. Thus, the orbital ES provides a "fingerprint" of the topological order, which can be used to identify the emergent topological phase in a microscopic Hamiltonian [36, 41–44].

As a model FQH state, the RR_3 parafermion state can be represented by its highest-density root configuration pattern of "1110011100... 11100111", corresponding to a generalized Pauli principle of "no more than three electrons in five consecutive orbitals" [62–64]. Consequently, the orbital ES depends on the number of electrons in the partitioned subsystem [71]. In Fig. 3, we show the orbital ES of three distinct partitions for system size $N_e = 36$ for Coulomb GS. For $3n$ electrons in subsystem (Fig. 3(a)), the leading ES displays the multiplicity-pattern $1, 1, 3, 6, 12$ in the first five angular momentum sectors $\Delta L_z^A = 0, 1, 2, 3, 4$. For $3n + 1$ or $3n + 2$ electrons in subsystem (Fig. 3(b-c)), the ES shows the multiplicity-pattern of $1, 2, 5, 9$ in the $\Delta L = 0, 1, 2, 3$ momentum sectors. The above characteristic multiplicity-patterns of the low-lying ES agree with the predicted edge excitation spectrum of the RR_3 state obtained either from its associated CFT, or the "≤ 3 in 5" exclusion statistics rule [71].

In addition, we vary the Haldane pseudopotentials $\mathcal{V}^1(1)$ and $\mathcal{V}^1(3)$ (keeping all others at their Coulomb-interaction values), and map out an ES-gap diagram which illustrates the robustness of the FQH state as the interaction param-

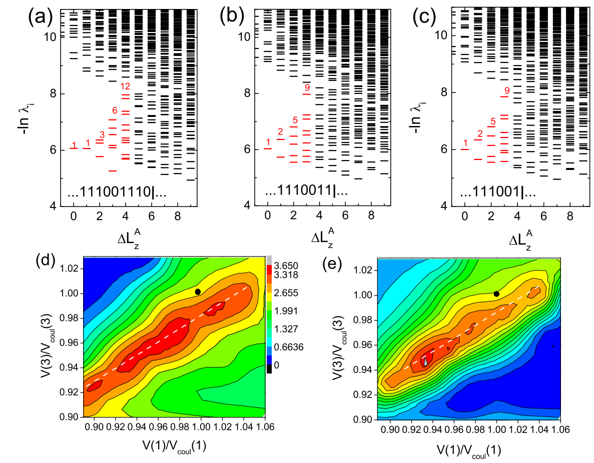

FIG. 3: (a-c) The low-lying orbital ES of $N_e = 36$ are shown for three different partitions. The lower ES level counting in the sector $\Delta L_z^A = 0, 1, 2, 3, 4$ are labeled by color, where $\Delta L_z^A = L_z^A - L_{z,min}^A$ with $L_{z,min}^A$ as the quantum number where the primary field occurs. The entanglement gap of orbital ES of $N_e = 24$ is shown for partition (d) with $3n$ electrons and (e) with $3n+1$ electrons in the subsystem as a function of pseudopotential $\mathcal{V}^1(1)/\mathcal{V}^1_{Coul}(1)$ and $\mathcal{V}^1(3)/\mathcal{V}^1_{Coul}(3)$, where $\mathcal{V}^1_{Coul}(l)$ are the Coulomb values of pseudopotentials. The black point corresponds to the Coulomb point.

eters are changed[65–68]. In Fig. 3, we plot the entanglement gap (for the lowest-L^z ES level)[36, 54] as a function of $\mathcal{V}^1(1)/\mathcal{V}^1_{Coul}(1)$ and $\mathcal{V}^1(3)/\mathcal{V}^1_{Coul}(3)$, where $\mathcal{V}^1_{Coul}(l)$ are the Coulomb values of pseudopotentials. We find that the entanglement gap is robust in a region centered at an approximately-fixed $\mathcal{V}^1(1)/\mathcal{V}^1(3)$ ratio (indicated by the white line). Away from that, for the regime $\mathcal{V}^1(1)/\mathcal{V}^1_{Coul}(1) < 0.92$ and $\mathcal{V}^1(3)/\mathcal{V}^1_{Coul}(3) > 0.98$, we find a rapid drop of the entanglement gap indicating a quantum phase transition. We have also studied the effect of the ES of modifying the Coulomb interaction with a realistic layer width (b) [71], and find that the RR_3 state persists until $b/l_B \sim 2$, which is qualitatively consistent with the results of varying $\mathcal{V}^1(1)$ and $\mathcal{V}^1(3)$.

Topological Entanglement Entropy.— For a two-dimensional gapped topologically-ordered state, the dependence of the entanglement entropy $S_A(l_A)$ of the subsystem A on the finite boundary-cut length l_A has the form $S_A(l_A) = \alpha l_A - \gamma$, where TEE γ is related to the total quantum dimension $\mathcal{D}$ by $\gamma = \ln \mathcal{D}$ [34, 35]. We have extracted the TEE using our largest system, $N_e = 36$ [71]. The TEE obtained was $\gamma = 1.491 \pm 0.091$, consistent with the theoretically-predicted value $\gamma = \ln \mathcal{D} = \ln \sqrt{5(1+\phi^2)} \approx 1.447$ for the RR_3 state, where each non-Abelian Fibonacci anyon quasiparticle contributes an individual quantum dimension $d_F = \phi = (\sqrt{5}+1)/2$ (ϕ denotes the Golden Ratio). The appearance of $d_F = \phi$ is a signal of the emergence of Fibonacci anyon quasiparticles, and arises because two Fibonacci quasiparticles may fuse either into the identity or into a single Fibonacci quasiparticle [47]. This exotic property makes Fibonacci quasiparticles capable of universal quantum computation [17].

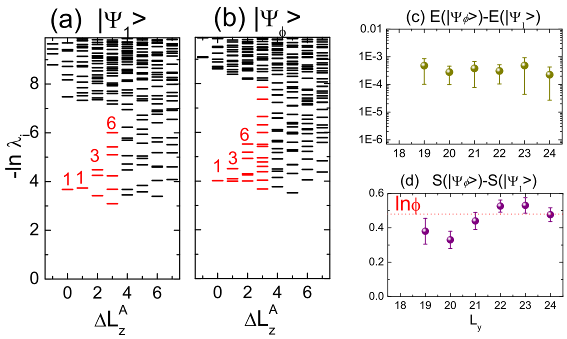

FIG. 4: (a-b) The low-lying orbital ES of Ψ_1 and $|\Psi_\phi\rangle$ by setting $L_y = 24l_B$. $|\Psi_{1(\phi)}\rangle$ denotes the GS with identity $\mathbb{1}$ (Fibonacci ϕ) anyonic quasiparticle. (c) Energy difference and (d) entropy difference between $|\Psi_1\rangle$ and $|\Psi_\phi\rangle$, obtained from infinite DMRG on cylinder geometry with varying L_y. The error bars are determined based on results from ten different infinite DMRG calculations for each sector[71].

Topological Degeneracy on the infinite cylinder.— Topologically-ordered states have characteristic GS degeneracies on compactified spaces. To access the different topological sectors at $\nu = 13/5$, we implemented the infinite-size DMRG in cylinder geometry with a finite circumference L_y [44, 69, 71]. For each value of L_y, we repeatedly calculated GSs using different random initializations for the infinite DMRG optimization. We found that each infinite DMRG simulation converged to one of the two states: $|\Psi_1\rangle$ and $|\Psi_\phi\rangle$. These states are distinguishable by their orbital ES as shown in Fig. 4: $|\Psi_1\rangle$ has the same ES structure as in Fig. 3(a-c), which matches the identity sector with root configuration "$\ldots 0111001110 \ldots$". On the other hand, $|\Psi_\phi\rangle$ shows the ES multiplicity pattern $1, 3, 6, 13, \ldots$, which identifies the spectrum as that of the Fibonacci non-Abelian sector with root configuration "$\ldots 1010110101 \ldots$" [71, 78]. Furthermore, these two groundstates are indeed energetically degenerate, with an energy-difference per electron of less than 0.0002 with $L_y = 24l_B$, while the entropy difference between these two states is around $\Delta S \approx \ln\phi \approx 0.48$, consistent with the quantum dimension of the Fibonacci quasiparticle. Combining this with the fivefold center-of-mass degeneracy, we have obtained all the 10 predicted degenerate RR_3 GSs on infinite cylinder (or torus).

Summary and discussion.— We have presented what we believe to be compelling evidence that the essence of the Coulomb-interaction ground states at $\nu = 13/5$ and $12/5$ is indeed captured by the parafermion $k = 3$ Read-Rezayi state RR_3, in which quasiparticles obey non-Abelian "Fibonacci-anyon" statistics. The neutral excitation gap is found to be a finite value $\Delta_n \approx 0.012e^2/l_B$ in the thermodynamic limit. Results for the entanglement spectrum "fingerprint" and the value of the topological entanglement entropy show that the edge structure and bulk quasiparticle statistics are consistent with the prediction bases on the RR_3 state. Additionally, we find two topologically-degenerate groundstate sectors on the infinite cylinder, respectively corresponding to the identity and the Fibonacci anyonic quasiparticle, which fully confirms the RR_3 state, without input of any features (such as shift) taken from the model wavefunction, that might have biased the calculation. The current work opens up a number of directions deserving further exploration. For example, while the FQH $\nu = 12/5$ state has been observed in experiment, there is no evidence of a FQH phase at $\nu = 13/5$ in the same systems [5, 8]. So far it is not clear whether this absence is due to a broken particle-hole symmetry from Landau level mixing, or other asymmetry effects such as differences in the quantum wells [7]. Our numerical studies suggest that the outlook for the existence of such a state at $13/5$ is promising, and some positive signs of this may have already been observed very recently [70]. Numerical studies may also further suggest how various other exotic FQH states in the second Landau level at different filling-factors may be stabilized.

Note added.— After the completion of this work, we became aware of overlapping results in Refs. [79].

WZ thanks Z. Liu for fruitful discussion, N. Regnault and A. Wójs for useful comments. We also thank X. G. Wen for stimulating discussion and M. Zaletel, R. S. K. Mong, F. Pollamann for private communication prior to publication. This work is supported by the U.S. Department of Energy, Office of Basic Energy Sciences under grants No. DE-FG02-06ER46305 (WZ, DNS) and DE-SC0002140 (FDMH), and the National Science Foundation through the grant DMR-1408560 (SSG). FDMH also acknowledges support from the W. M. Keck Foundation. WZ also acknowledges the support from MRSEC DMR-1420541 and PREM DMR-1205734 for a visit to Princeton where this work was completed.

[1] D. C. Tsui, H. L. Stormer, and A. C. Gossard, Phys. Rev. Lett. **48**, 1559 (1982).
[2] R. B. Laughlin, Phys. Rev. Lett. 50, 1395 (1983).
[3] R. Willett, J. P. Eisenstein, H. L. Stormer, D. C. Tsui, A. C. Gossard, and J. H. English, Phys. Rev. Lett. 59, 1776 (1987).
[4] W. Pan, J.-S. Xia, V. Shvarts, D. E. Adams, H. L. Stormer, D. C. Tsui, L. N. Pfeiffer, K. W. Baldwin, and K. W. West, Phys. Rev. Lett. 83, 3530 (1999).
[5] J. S. Xia, W. Pan, C. L. Vicente, E. D. Adams, N. S. Sullivan, H. L. Stormer, D. C. Tsui, L. N. Pfeiffer, K. W. Baldwin, and K. W. West, Phys. Rev. Lett. 93, 176809 (2004),
[6] H. C. Choi, W. Kang, S. Das Sarma, L. N. Pfeiffer, K. W. West, Phys. Rev. B **77**, 081301(R) (2008).
[7] W. Pan, et al., Phys. Rev. B **77**, 075307 (2008).
[8] A. Kumar, G. A. Csathy, M. J. Manfra, L. N. Pfeiffer and K. W. West, Phys. Rev. Lett. 105, 246808 (2010).
[9] I. P. Radu, J. B. Miller, C. M. Marcus, M. A. Kastner, L. N. Pfeiffer, K. W. West, Science **320**, 899 (2008).
[10] M. Dolev, M. Heiblum, V. Umansky, A. Stern, and D. Mahalu, Nature **452**, 829 (2012).
[11] R. L. Willett, C. Nayak, K. Shtengel, L. N. Pfeiffer, and K. W. West, Phys. Rev. Lett. **111**, 186401 (2013).

[12] S. Baer, C. Rossler, T. Ihn, K. Ensslin, C. Reichl and W. Wegscheider, Phys. Rev. B **90**, 075403 (2014).

[13] C. Zhang, C. Huan, J. S. Xia, N. S. Sullivan, W. Pan, K. W. Baldwin, K. W. West, L. N. Pfeiffer, and D. C. Tsui, Phys. Rev B **85**, 241302(R) (2012)

[14] G. Moore and N. Read, Nucl. Phys. B **360**, 362 (1991).

[15] M. Greiter, X. G. Wen and F. Wilczek, Phys. Rev. Lett. **66**, 3205 (1991).

[16] N. Read and E. Rezayi, Phys. Rev. B **59**, 8084 (1999).

[17] C. Nayak, S. H. Simon, A. Stern, M. Freedman and S. D. Sarma, Rev. Mod. Phys. **80**, 1083 (2008).

[18] A. Y. Kitaev, Ann. Phys. **303**, 2 (2003).

[19] M. H. Freedman, M. Larsen, and Z. Wang, Commun. Math. Phys. **227**, 605 (2002).

[20] S. Das Sarma, M. Freedman and C. Nayak, Phys. Rev. Lett. **94**, 166802 (2005).

[21] L. Hormozi, G. Zikos, N. E. Bonesteel, and S. H. Simon, Phys. Rev. B **75**, 165310 (2007).

[22] N. E. Bonesteel, L. Hormozi, G. Zikos, and S. H. Simon, Phys. Rev. Lett. **95**, 140503 (2005).

[23] R. S. K. Mong, D. J. Clarke, J. Alicea, N. H. Lindner, P. Fendley, C. Nayak, Y. Oreg, A. Stern, E. Berg, K. Shtengel, and M. P. A. Fisher, Phys. Rev. X **4**, 011036 (2014).

[24] A. Vaezi and M. Barkeshli, Phys. Rev. Lett. **113** 236804 (2014).

[25] E. H. Rezayi and N. Read, Phys. Rev. B **79**, 075306 (2009).

[26] F. D. M. Haldane, Phys. Rev. Lett. **51**, 605 (1983).

[27] B. I. Halperin, Phys. Rev. Lett. **52**, 1583 (1984).

[28] J. K. Jain, *Composite Fermions*, (Cambridge Univeristy Press, Cambridge, England, 2007).

[29] P. Bonderson and J. K. Slingerland, Phys. Rev. B **78**, 125323 (2008).

[30] P. Bonderson, A. E. Feiguin, G. Moller and J. K. Slingerland, Phys. Rev. Lett. **108**, 036806 (2012).

[31] G. J. Sreejith, C. Toke, A. Wojs and J. K. Jain, Phys. Rev. Lett. **107**, 086806 (2011).

[32] G. J. Sreejith, Y.-H. Wu, A. Wojs and J. K. Jain, Phys. Rev. B **87**, 245125 (2013).

[33] A. Wojs, Phys. Rev. B **80**, 041104(R) (2009).

[34] A. Kitaev and J. Preskill, Phys. Rev. Lett. **96**, 110404 (2006).

[35] M. Levin and X.-G. Wen, Phys. Rev. Lett. **96**, 110405 (2006).

[36] H. Li and F. D. M. Haldane, Phys. Rev. Lett. **101**, 010504 (2008).

[37] Y. Zhang, T. Grover, A. Turner, M. Oshikawa and A. Vishwanath, Phys. Rev. B **85**, 235151 (2012).

[38] X. G. Wen, Int. J. Mod. Phys. B **4**, 239 (1990).

[39] X. G. Wen, Advances in Physics **44**, 405 (1995).

[40] M. Haque, O. Zozulya, and K. Schoutens, Phys. Rev. Lett. **98**, 060401 (2007).

[41] A. M. Lauchli, E. J. Bergholtz, J. Suorsa and M. Haque, Phys. Rev. Lett. **104**, 156404 (2010).

[42] Z. Papic, B. A. Bernevig, and N. Regnault, Phys. Rev. Lett. **106**, 056801 (2011).

[43] L. Cincio and G. Vidal, Phys. Rev. Lett. **110**, 067208 (2013).

[44] M. P. Zaletel, R. S. K. Mong, F. Pollmann, Phys. Rev. Lett. **110**, 236801 (2013).

[45] H. H. Tu, Y. Zhang, and X. L. Qi, Phys. Rev. B **88**, 195412 (2013).

[46] H. C. Jiang, Z. H. Wang and L. Balents, Nat. Phys. **8**, 902 (2012).

[47] W. Zhu, S. S. Gong, F. D. M. Haldane, and D. N. Sheng, Phys. Rev. Lett. **112**, 096803 (2014).

[48] G. Fano, F. Ortolani, and E. Colombo, Phys. Rev. B **34**, 2670 (1986).

[49] M. Greiter, Phys. Rev. B **83**, 115129 (2011).

[50] S. R. White, Phys. Rev. Lett. **69**, 2863 (1992).

[51] T. Xiang, Phys. Rev. B **53**, 10445(R) (1996).

[52] N. Shibata and D. Yoshioka, Phys. Rev. Lett. **86** 5755 (2001).

[53] A. E. Feiguin, E. Rezayi, C. Nayak, and S. Das Sarma, Phys. Rev. Lett. **100**, 166803 (2008).

[54] J. Z. Zhao, D. N. Sheng and F. D. M. Haldane, Phys. Rev. B **83**, 195135 (2011).

[55] Z. X. Hu, Z. Papic, S. Johri, R. N. Bhatt, and P. Schmitteckert, Phys. Lett. A **376**, 2157 (2012).

[56] R. Morf, N. d'Ambrumenil, and B. I. Halperin, Phys. Rev. B **34**, 3037 (1986).

[57] The charged gap is out of the scope of current study.

[58] F. D. M. Haldane, and E. H. Rezayi, Phys. Rev. Lett. **54**, 237 (1985).

[59] S. M. Girvin, A. H. MacDonald and P. M. Platzman, Phys. Rev. Lett. **54**, 581 (1985).

[60] B. Yang, Z.-X. Hu, Z. Papic, and F. D. M. Haldane, Phys. Rev. Lett. **108**, 256807 (2012).

[61] While the obtained $\Delta_n \approx 0.012$ is close to the experimental estimated value (~ 0.016) at $\nu = 12/5$ [8], the asymmetry between $\nu = 12/5$ and $13/5$ in experiments may dependent on the details of systems and Landau level coupling, which is beyond the scope of current paper and left for the future study.

[62] E. J. Bergholtz and A. Karlhede, Phys. Rev. Lett. **94**, 026802 (2005).

[63] B. A. Bernevig and F. D. M. Haldane, Phys. Rev. Lett. **100**, 246802 (2008).

[64] B. A. Bernevig and F. D. M. Haldane, Phys. Rev. B **77**, 184502 (2008).

[65] M. R. Peterson, T. Jolicoeur, and S. Das Sarma, Phys. Rev. B **78**, 155308(2008).

[66] M. Storni, R. H. Morf, and S. Das Sarma, Phys. Rev. Lett. **104**, 076803 (2010).

[67] J. Biddle, M. R. Peterson, and S. Das Sarma, Phys. Rev. B **84**, 125141 (2011).

[68] K. Pakrouski, M. R. Peterson, T. Jolicoeur, V. W. Scarola, C. Nayak, and M. Troyer, Phys. Rev. X **5**, 021004 (2015).

[69] M. P. Zaletel, R. S. K. Mong, F. Pollmann and E. H. Rezayi, Phys. Rev. B **91**, 045115 (2015).

[70] J. Falson, D. Maryenko, B. Friess, D. Zhang, Y. Kozuka, A. Tsukazaki, J. H. Smet, and M. Kawasaki, Nat. Phys. **11**, 347 (2015).

[71] See Supplemental Material, which includes Ref. [72–77].

[72] D. Yoshioka, J. Phys. Soc. Jap. **55**, 885 (1986).

[73] T. T. Wu, and C. N. Yang, Phys. Rev. D, **77** 1018 (1977).

[74] R. E. Wooten, Bulletin of the American Physical Society (2015).

[75] O. S. Zozulya, M. Haque, K. Schoutens, and E. H. Rezayi, Phys. Rev. B **76**, 125310 (2007).

[76] B. Estienne, N. Regnault, B. A. Bernevig, Phys. Rev. Lett. **114**, 186801 (2015).

[77] I. McCulloch, arXiv.0804.2509.

[78] The ES results shown in this paper give an unambiguous confirmation of RR_3 state as the ground state at $\nu = 12/5$ and $13/5$. Based on this measurement, we can also exclude the possibility of the Jain CF state, because Jain state is expected to show $1, 2, 5, ...$ degeneracy pattern in ES.

[79] R. S. K. Mong, M. P. Zaletel, F. Pollmann and Z. Papic,, arXiv. 1505.02843.